

Supplementary Material

Promoting effects of indium doping Cu/CeO₂ catalyst for CO₂ hydrogenation to methanol

Marco A. Rossi^{†a}, Luiz H. Vieira^{‡a,c*}, Letícia F. Rasteiro^a, Marco A. Fraga^b, José M. Assaf^c and Elisabete M. Assaf^{a*}

^aSão Carlos Institute of Chemistry (IQSC), University of São Paulo (USP), Av. Trabalhador São-Carlense 400, CEP 13566-590, São Carlos, SP, Brazil.

^bNational Institute of Technology (INT/MCTIC), Av. Venezuela, 82/518, Saúde, CEP: 20081-312, Rio de Janeiro, RJ, Brazil.

^cSão Carlos Federal University, Chemical Engineering Department, Rod. Washington Luiz, km 235 – SP 310, CEP: 13565-905, São Carlos, SP, Brazil.

[†]*These authors contributed equally.*

^{*}*Corresponding authors:* lhvieira@ufscar.br; eassaf@iqsc.usp.br

Supplementary Tables

Table S1. Defined values for upper level, lower level, center points, and axial points for each one of the variables (pressure, temperature, and space velocity).

Variable	Lower	Lower	Centre	Upper	Upper
	Axial Point	Level	Points	Level	Axial Point
	(- a)	(-1)	(0)	(+1)	(+ a)
Pressure (MPa)	1.66	2	2.5	3	3.34
Temperature (K)	455.96	473	498	523	540.04
S. Velocity (L.g ⁻¹ .h ⁻¹)	3.95	6	9	12	14.05

Table S2. Crystalline phase composition for CuCe, CuCeIn5, and CuCeIn10 estimated by Rietveld refinement. as well as R_{wp} and GOF (goodness-of-fit) values.

Catalyst	Weight%		Molar%		R_{wp}	GOF
	CeO ₂	CuO	CeO ₂	CuO		
CuCe	73.0	27.0	55.6	44.4	5.25	3.74
CuCeIn5	71.2	28.8	53.3	46.7	5.33	3.73
CuCeIn10	73.0	27.0	55.6	44.4	5.27	3.87

Table S3. Chemical composition for Cu/CeO₂, Cu/CeO₂-5%In, and Cu/CeO₂-5%In analyzed by ED-XRF.

Catalyst	Elemental Composition (% molar)		
	Cu	Ce	In
CuCe	52.5	47.5	0.0
CuCeIn5	54.7	40.5	4.8
CuCeIn10	55.3	35.9	8.8

Table S4. CeO_2 lattice parameter and unit cell volume for CuCe, CuCeIn5, and CuCeIn10 catalysts calculated by Rietveld refinement, as well as R_{wp} and GOF (goodness-of-fit) values.

Catalyst	a_{CeO_2} (\AA)	V_{CeO_2} (\AA^3)
CuCe	5.424	159.60
CuCeIn5	5.414	158.70
CuCeIn10	5.401	157.59

Table S5. CuO lattice parameters and unit cell volume for CuCe, CuCeIn5, and CuCeIn10 catalysts calculated by Rietveld refinement, as well as R_{wp} and GOF (goodness-of-fit) values.

Catalyst	a_{CuO} (\AA)	b_{CuO} (\AA)	c_{CuO} (\AA)	β_{CuO} ($^\circ$)	V_{CuO} (\AA^3)
CuCe	4.694	3.424	5.133	99.47	81.38
CuCeIn5	4.699	3.430	5.137	99.51	81.70
CuCeIn10	4.698	3.434	5.141	99.51	81.83

Table S6. Pore volume obtained by N_2 physisorption for Cu/CeO₂, CuCeO₂-5%In, and Cu/CeO₂-10%In catalysts.

Catalyst	Pore total volume ($\text{cm}^3 \cdot \text{g}^{-1}$)	Mesopore volume ($\text{cm}^3 \cdot \text{g}^{-1}$) ^a	Micropore volume ($\text{cm}^3 \cdot \text{g}^{-1}$) ^b
CuCe	0.060	0.055	0.005
CuCeIn5	0.049	0.046	0.003
CuCeIn10	0.048	0.045	0.003

^aObtained using BJH isotherm model.

^bObtained using the t-plot method.

Table S7. Core level binding energies for cerium and indium. The standard values were obtained from the Handbook of X-ray Photoelectron Spectroscopy.

Catalyst	Binding Energy (eV)			
	Ce ⁴⁺ 3d ^{5/2}	Ce ³⁺ 3d ^{5/2}	In ³⁺ 3d ^{5/2}	In ³⁺ 3d ^{5/2} a
Standard	~881.8	~881.0	~444.3	~443.8
CuCe	882.8	881.1	-	-
CuCeIn5	883.1	881.3	444.85	444.43
CuCeIn10	882.7	881.1	444.40	444.0

^aIn³⁺ in non-stoichiometric oxides.

Table S8. Apparent activation energies for CH₃OH and CO formation in the catalysts, calculated from Arrhenius plot in Figures 6d and 6e.

Catalysts	E _a CH ₃ OH (kJ.mol ⁻¹)	E _a CO (kJ.mol ⁻¹)
CuCe	44.0	73.2
CuCeIn5	40.7	80.4
CuCeIn10	49.2	83.9

Table S9. Experimental matrix designed by central composite methodology and results of CO₂ conversion rate and selectivity for CH₃OH, CO, CH₄, and C₂H₆ products under different conditions for Cu/CeO₂-5%In.

Assay	P (MPa)	T (K)	S. Velocity (L.g ⁻¹ .h ⁻¹)	X _{CO2} (%)	S _{CH3OH} (%)	S _{CO} (%)	S _{CH4} (%)	S _{C2H6} (%)
1	2	473	6	0.9	72.7	26.5	0.5	0.3
2	2	473	12	0.6	73.8	25.3	0.4	0.5
3	2	523	6	6.0	32.6	66.8	0.5	0.1
4	2	523	12	3.7	34.8	64.7	0.4	0.1
5	3	473	6	1.7	78.5	20.6	0.5	0.4
6	3	473	12	1.0	80.1	19.2	0.3	0.4
7	3	523	6	7.7	37.5	61.9	0.5	0.1
8	3	523	12	4.7	42.2	57.3	0.4	0.1
9	1.66	498	9	1.5	50.9	48.5	0.5	0.1
10	3.34	498	9	3.0	62.4	37.1	0.4	0.1
11	2.5	455.96	9	0.3	98.8	0.0	0.2	1.0
12	2.5	540.04	9	7.9	30.1	69.2	0.7	0.0
13	2.5	498	3.95	3.3	55.4	44.0	0.5	0.1
14	2.5	498	14.05	1.4	61.4	37.9	0.5	0.2
15	2.5	498	9	1.8	60.3	39.0	0.5	0.2
16	2.5	498	9	1.9	59.4	40.0	0.4	0.2
17	2.5	498	9	1.8	59.8	39.6	0.4	0.2

Supplementary Note 1: Small amounts of ethane (< 1%) were identified between products. We speculate that this can be related to the increased stabilization of CO intermediates in In-promoted catalysts, as observed by DRIFTS analysis, which can be thermally coupled even in the absence of iron-based catalysts (generally used for the process). The very low selectivity makes this not relevant for the process, and more efforts to try to elucidate this will not lead to advances in the field.

Table S10. Main and interaction effects calculated for pressure, temperature and space velocity using the CuCeIn5 catalyst.

Parameters	Effects	Error	Standardized Effects (t)	Significance ^a
Pressure (X1)	6.4057	0.2440	26.2485	Yes
Temperature (X2)	-40.0589	0.2440	-164.1496	Yes
S. Velocity (X3)	2.8836	0.2440	11.8163	Yes
X1*X2	0.0500	0.3189	0.1568	No
X1*X3	0.7500	0.3189	2.3522	No
X2*X3	1.0500	0.3189	3.2931	No

^aAnalyzed considering the critical effect equal to 1.37 with a standardized value of 4.303.

Table S11. Analysis of variance (ANOVA) for the quadratic model fit to the experimental data.

Variation Source	Sum of Squares	Degrees of Freedom	Quadratic Mean	F- Value	p-Value
Regression	5.7291x10 ³	9	636.5698	114.6009	9.1983x10 ⁻⁷
Residual	38.8827	7	5.5547	-	-
Lack-of-fit	38.476	5	7.6952	37.8453	0.0259
Pure Error	0.4067	2	0.2033	-	-
SS _{Total}	5.768x10 ³	16			
R ²	0.9933				
Explainable R ²	0.9999				

Table S12. Overview of CO₂ hydrogenation catalysts in the literature.

Catalyst	H ₂ :CO ₂ ratio	P (MPa)	T (K)	GHSV (L/g _{cat} .h)	X _{CO₂} (%)	S _{CH₃OH} (%)	S _{CO} (%)	S _{HC} (%) ^f	STY _{CH₃OH} (mmol/g _{cat} .h) ^g	Ref.
In ₂ O ₃	3:1	4.0	543	15	1.1	54.9	-	-	0.78	1
In ₂ O ₃	3:1	4.0	603	15	7.1	39.7	-	-	3.69	1
Cu/ZrO ₂	3:1	0.1	493	75	0.53	19.8	80.2	-	0.70	2
Cu/TiO ₂	3:1	0.1	493	5.6	0.54	13.8	83.6	-	0.03	2
Cu/ZnO/ZrO ₂	3:1	1.0	473	8.8	3.2	64.7	-	-	2.43	3
Cu/CeO ₂	3:1	3.0	483	3.0	2.4	77.9	-	-	0.50	4
CuPd/CeO ₂	3:1	3.0	483	3.0	4.3	52.4	-	-	0.61	4
Cu/ZnO/Al ₂ O ₃	3:1	3.0	503	2.4	18.7	43.0	-	-	2.15	5
Cu/ZnO/ZrO ₂	3:1	3.0	503	2.4	19.3	48.6	-	-	2.51	5
Cu/ZnO/ZrO ₂ /Al ₂ O ₃	3:1	3.0	503	2.4	23.2	60.3	-	-	3.75	5
Cu/MgO/Al ₂ O ₃	3:1	2.0	523	2.0	~3	~17	-	-	0.80	6
Cu/CeO ₂ -CM ^a	3:1	3.0	523	30	1.0	53	-	-	1.40	7
Cu/CeO ₂ -cube	3:1	3.0	523	30	0.9	25	-	-	0.60	7
Cu/CeO ₂ -sphere	3:1	3.0	523	30	1.5	52	-	-	2.00	7
Cu/CeO ₂ -rod	3:1	3.0	523	30	1.2	43	-	-	1.40	7
Cu/CeO ₂ -FSP ^b	3:1	3.0	523	30	1.4	48	-	-	1.90	7

Cu/CeO ₂ -CP ^c	3:1	3.0	523	30	1.3	49	-	-	1.70	7
Cu/CeO ₂ -DP ^d	3:1	3.0	523	30	1.6	50	-	-	2.10	7
Cu-SiO ₂	3:1	3.0	523	60	1.1	16	-	-	1.10	7
CuCe	3:1	3.0	523	8.0	9.4	35.4	64.2	0.4	2.74	This work
Cu/CeIn5	3:1	3.0	548	8.0	9.7	46.4	52.8	0.8	3.70	This work
CuCeIn10	3:1	3.0	548	8.0	10.0	54.6	44.1	1.3	4.47	This work
CuCeIn5 ^e	3:1	3.0	456	12	0.7	99.3	0.0	0.7	0.85	This work

a. commercial ceria powder (<25 nm, Sigma-Aldrich).

b. prepared by a flame spray pyrolysis method.

c. prepared by a coprecipitation method.

d. prepared by deposition–precipitation on the commercial ceria powder (<25 nm, Sigma-Aldrich).

e. under the best conditions to promote CH₃OH selectivity determined through chemometric analysis.

f. selectivity to hydrocarbons.

g. methanol space-time yield.

Supplementary Figures

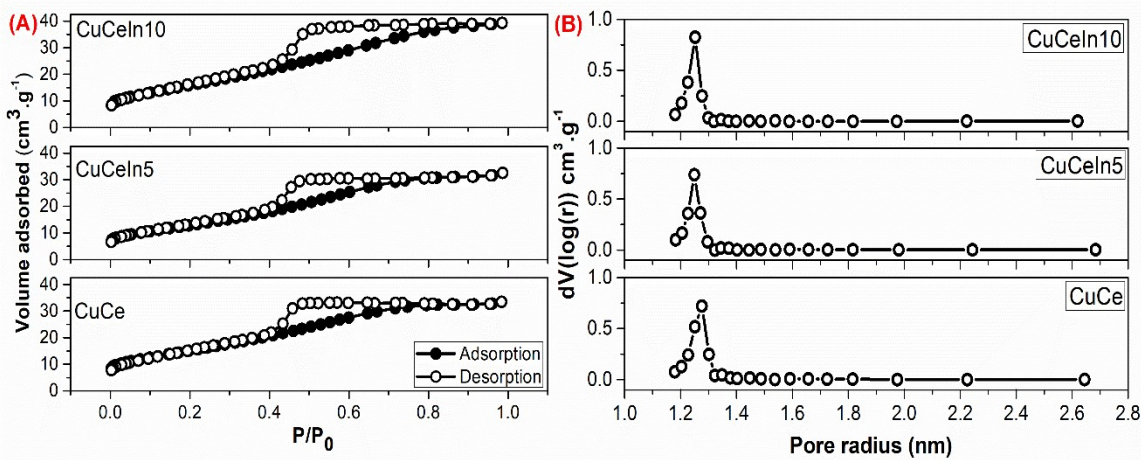


Figure S1. (A) N₂ adsorption/desorption isotherms and (B) pore size distribution for CuCe, CuCeIn5, and CuCeIn10 materials. All materials presented a type IV isotherm with hysteresis loop due to capillary condensation typical of mesoporous materials and similar pore size distribution.

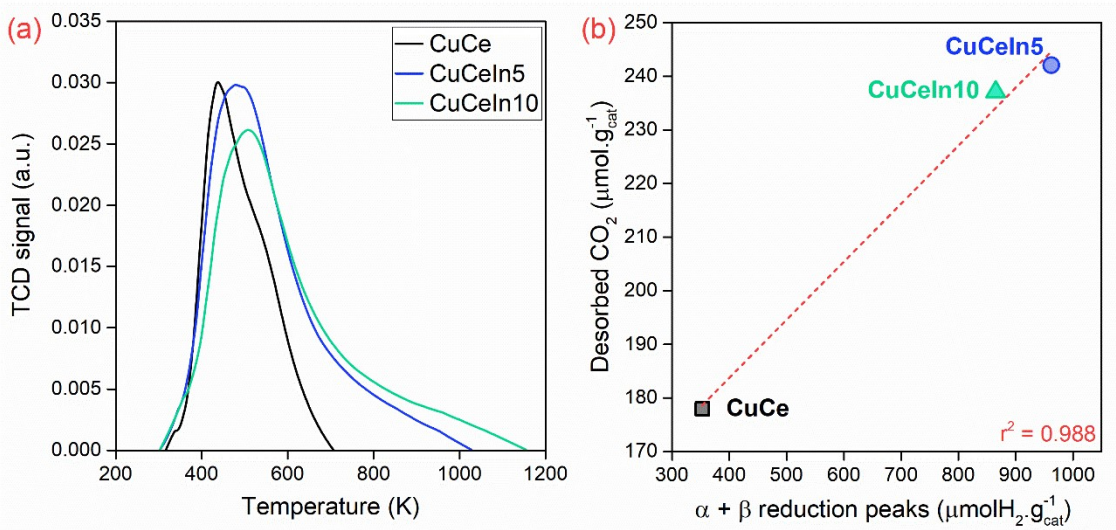


Figure S2. (a) CO₂ temperature-programmed desorption profiles for CuCe, CuCeIn5, and CuCeIn10 catalysts. (b) Correlation between $\alpha + \beta$ reduction peaks in H₂-TPR and the amount of CO₂ desorb during CO₂-TPD.

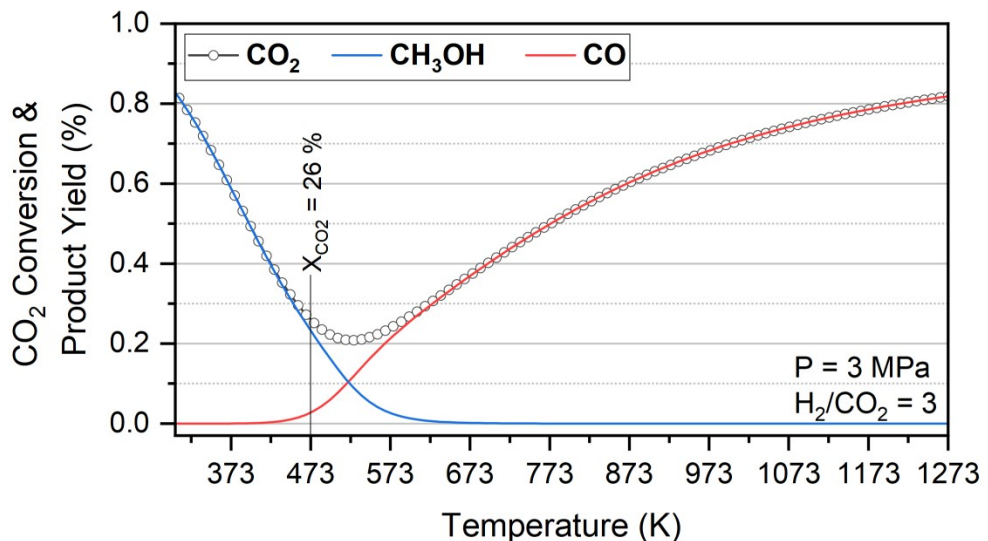


Figure S3. Thermodynamic equilibrium data. CO₂ conversion and yields for CH₃OH and CO during hydrogenation at 3.0 MPa with a CO₂:H₂ = 1:3 at the initial state.

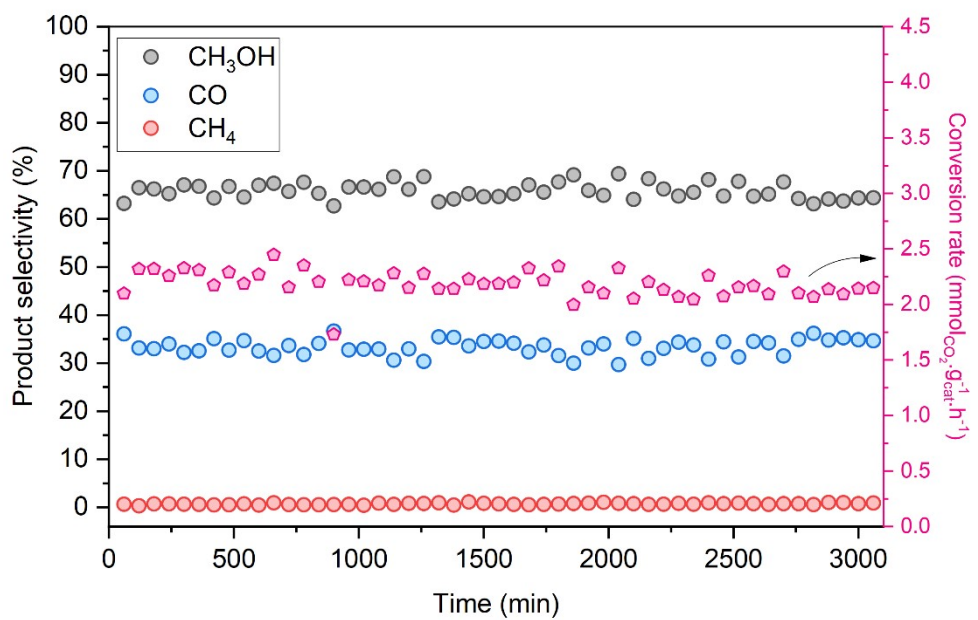


Figure S4. Stability test during CO₂ hydrogenation over CuCeIn5. Reaction conditions: 498 K, 3.0 MPa, 8 L.g⁻¹.h⁻¹, CO:H₂ = 1:3.

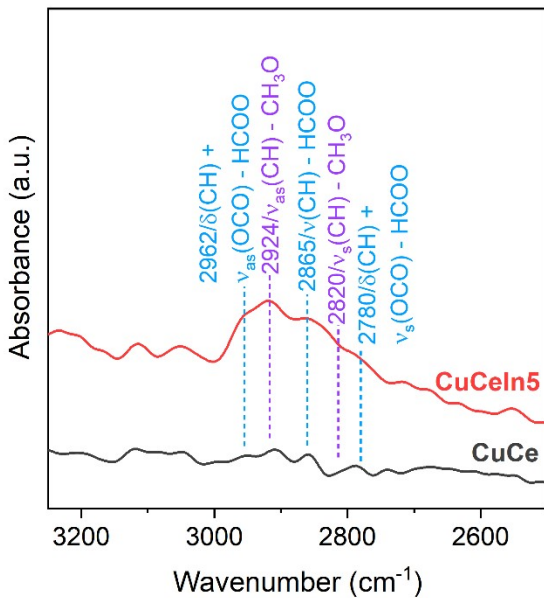


Figure S5. *In situ* DRIFTS analysis of CuCe and CuCeIn5 catalysts after CO₂ flow for 30 min followed by H₂ flow for additional 30 min at 473 K.

References

- 1 K. Sun, Z. Fan, J. Ye, J. Yan, Q. Ge, Y. Li, W. He, W. Yang and C. J. Liu, *J. CO₂ Util.*, 2015, **12**, 1–6.
- 2 S. Kattel, B. Yan, Y. Yang, J. G. Chen and P. Liu, *J. Am. Chem. Soc.*, 2016, **138**, 12440–12450.
- 3 F. Arena, G. Italiano, K. Barbera, S. Bordiga, G. Bonura, L. Spadaro and F. Frusteri, *Appl. Catal. A Gen.*, 2008, **350**, 16–23.
- 4 E. J. Choi, Y. H. Lee, D. W. Lee, D. J. Moon and K. Y. Lee, *Mol. Catal.*, 2017, **434**, 146–153.
- 5 C. Li, X. Yuan and K. Fujimoto, *Appl. Catal. A Gen.*, 2014, **469**, 306–311.
- 6 V. D. B. C. Dasireddy, N. S. Štefančič, M. Huš and B. Likozar, *Fuel*, 2018, **233**, 103–112.
- 7 J. Zhu, Y. Su, J. Chai, V. Muravev, N. Kosinov and E. J. M. Hensen, *ACS Catal.*, 2020, **10**, 11532–11544.